Macalester Journal of Physics and Astronomy

Volume 9
Issue 1 *Spring 2021*

Article 2

May 2021

Virtual Prototyping of Liquid Lithium Divertor Concepts

Brennan Arnold
Macalester College, barnold1@macalester.edu

Virtual Prototyping of Liquid Lithium Divertor Concepts

Abstract

A tokamak divertor must withstand power deposition in excess of 10 MW/m^2 in steady state and much higher in disruptions, enough to destroy nearly any material. In order to handle this extreme heat, there is some interest in using liquid metal flows to continually renew the divertor surface. In this paper, we examine an idea for a divertor with a porous surface that allows liquid lithium flowing through the divertor to percolate to the plasma facing surface. This idea is complicated by magnetohydrodynamic drag, where the stong magnetic fields in the tokamak cause the lithium to flow too slowly to carry away all the heat. In order to speed the lithium up, we apply an electric current across the channel.

We simulate the system using a simplified model in ANSYS, which we validate through comparisons to several analytical results. The simulation suggests that the design can handle the power applied a divertor. We examine the amount of current that must be applied to achieve sufficient lithium velocities, and begin to probe the effect of channel geometries on divertor efficiency.

I. INTRODUCTION

In principle, fusion is an ideal way to generate clean, renewable energy. It could generate continuous energy using very small amounts of fuel and leaving behind no radioactive waste. However, fusion is very difficult to achieve on earth due to the extreme conditions that need to be maintained. A tokamak is a device that uses magnetic fields to confine plasmas and maintain these extreme conditions for fusion.

In the tokamak, the plasma is shaped into a torus by strong electromagnets and a current is driven around the toroidal direction. This current generates a magnetic field which, in conjunction with the field generated by the magnets, maintains the plasma confinement. On the outside of the plasma, near the wall, there is a cold, contaminated layer of plasma. In order to keep the core plasma hot and pure enough for fusion to occur, this outer layer should not be allowed to mix with the core. Some tokamaks deal with the scrape-off layer by shaping the magnetic fields to direct it onto a divertor, which is plasma-facing component designed to withstand continuous deposition of the edge plasma. A divertor may need to absorb 10s of megawatts of power in steady-state operation and much more during a disruption[1]. Most materials would be destroyed by this amount of continuous power deposition, so a divertor needs some way to quickly shuttle the energy away from the plasma facing surface.

There are some designs for divertors with liquid lithium surfaces. These could be more resilient than typical solid divertors because the surface is being continuously renewed. One major issue with liquid divertors is that it's difficult to control a free surface flow, especially of a conductive fluid in a strong magnetic field.

In this project, we perform preliminary analysis of a porous delivery system, in which liquid lithium can move from an interior channel flow to the plasma facing surface through a porous surface. This system has the advantages of a self-renewing divertor surface, but without the control disadvantages of a free surface flow.

One of the major issues with this idea is magnetohydrodynamic (MHD) drag in the channel. Since the lithium is conductive, there is a current induced in the liquid as it passes through the magnetic field. Then, since the current is perpendicular to the magnetic field, there's a Lorentz force on this induced current. This Lorentz force always opposes the direction of the flow, so it is effectively a drag force that causes liquid metal to move very slowly in a tokamak's strong magnetic field. (Figure 1) However, liquid lithium in a divertor needs to move quickly so it can remove all the heat applied to the channel.

Our strategy to overcome the MHD drag is to apply a current to the channel against the induced current. The Lorentz force on the applied current is in the direction of the flow, therefore accelerating the flow. By increasing the applied current, we can increase the rate at which heat is shuttled away from the divertor surface, improving the performance of the divertor.

In this project, we build a simple virtual model of a single channel in this divertor concept. The goal is to create a generic model that can be then be modified to make engineering decisions for a specific tokamak for which a liquid lithium divertor is being considered. In order to ensure that the physics is working properly in our model, we use a very simple geometry and compare to analytical MHD solutions. This also allows us to determine what mesh densities are required to achieve a balance between solution fidelity and convergence speed. We do some preliminary testing of various currents and channel geometries to determine whether the concept is capable of removing the imposed heat load and keeping the temperature of the channel down to 450°C, which will minimize the consequences of lithium contamination in the plasma.[2]

Important variables that are used throughout this paper are defined in Table I.

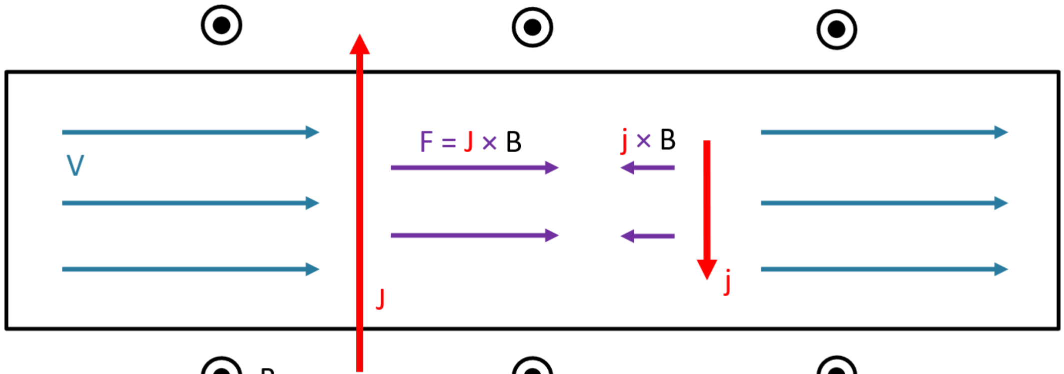

FIG. 1: A magnetic field pointing out of the page induced a downward current (j) in conductive fluid flowing to the right. This current creates a drag force opposing the direction of the flow. Passing a larger current (J) upwards through the fluid creates a force in the direction of the flow, increasing the velocity.

TABLE I: Definitions of all variables used throughout this paper

Symbol	Meaning	Units	Equation
B_0	magnitude of applied magnetic field	T	
a	half-width of the lithium channel	m	
b	half-height of the lithium channel	m	
σ	conductivity of lithium	$\mathrm{S \cdot m^{-1}}$	
η	dynamic viscosity of lithium	$\mathrm{Pa \cdot s}$	
ρ	density of lithium	$\mathrm{kg \cdot m^{-3}}$	
v_0	average velocity	$\mathrm{m \cdot s^{-1}}$	
v_1	average velocity on the $y = b$ plane	$\mathrm{m \cdot s^{-1}}$	
I	total current	$\mathrm{a \cdot m^{-1}}$	
M	Hartmann number		$B_0 a\sqrt{\sigma/\eta}$
J	nondimensionalized current		$\mu_0 I/B_0$
P	nondimensionalized external force on the lithium		$2a\rho g\mu_0/B_0^2$
L	nondimensionalized channel height		b/a
Q	nondimensionalized mass flow rate		$v_0\,(8\mu_0 b\sigma/M)$
J^*	J factor		J/P

II. MODEL

The virtual model built in ANSYS CFX, a commercial software with fluid dynamics capabilities, is shown is Figure 2. The channel is filled with liquid lithium which is being pulled in the $+x$ direction by gravity. An external 10T magnetic field is applied in the $+z$ direction and we apply current through the channel in the $+y$ direction. For the remainder of this paper, I will refer to the amount of current passed through the channel by its "J factor,"

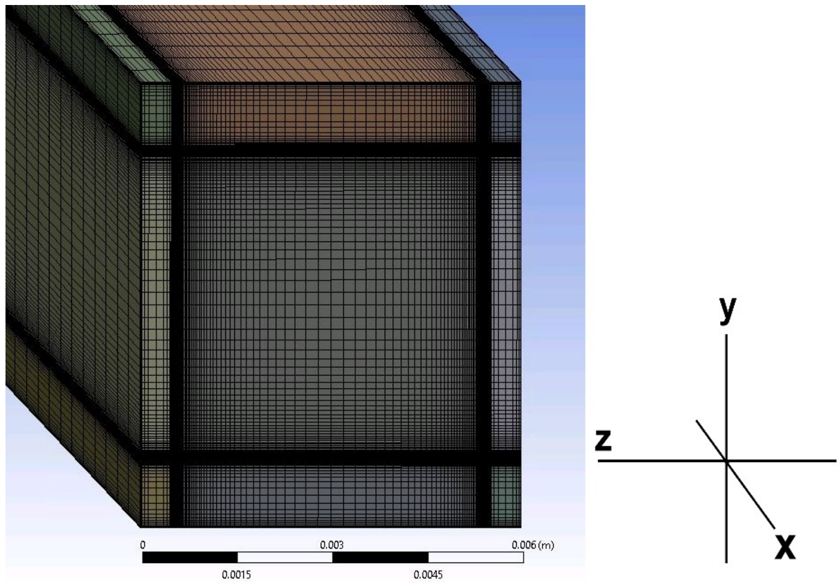

FIG. 2: The ANSYS model with the mesh displayed. The mesh is coarse in the walls and at the middle of the liquid channel where high resolution is not required to achieve a good solution. The mesh density is much higher near the interfaces between the liquid domain and walls where boundary layers are expected and need to be resolved.

J^*. This is a convenient way to scale the current that indicates how much of the velocity of the lithium is due to the current, compared to the velocity due to gravity. A J factor of 1 indicates that enough current is being passed through to double the average velocity of the lithium, and a J factor of 5 indicates that the current responsible for 5/6 of the velocity.

The liquid domain is bounded by a pair of insulating walls at $z = \pm a$mm and a pair at $y = 0, 2b$. For the purposes of these simulations, a is fixed at 2.5mm and we varied b when investigating the effect of different aspect ratios ($a : b$) on the heat transfer. We also changed the conductivity of the walls at $y = 0, 2b$ to match to different analytical results. The simulated portion of the channel is 1m long.

This simple setup captures most of the interesting properties of the porous delivery system. By making the assumption that heat is transferred from the outer edge of the porous surface into the main lithium flow only through conduction, rather than by any motion of the fluid in the pores, we bypass the need to explicitly allow lithium from inside the channel to travel through the wall. So to complete the model, we apply a heat flux to one of the sides parallel to the external magnetic field, which represents the porous surface on the actual divertor.

A. Heat flux model

To simulate the heat deposited on the divertor by the plasma, we use a Gaussian heat flux model with a correction that depends on temperature. The Gaussian has a peak heat flux of $10MW/m^2$ near the inlet. This profile is shown in Figure 3.

At low temperature, the channel absorbs all of this heat, but at higher temperatures, the lithium is more likely to evaporate off of the surface, so less of the heat is absorbed. To

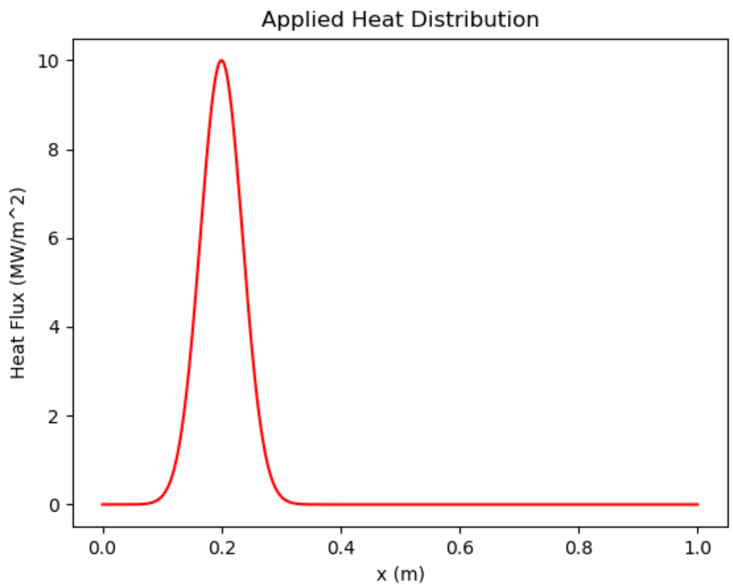

FIG. 3: A gaussian heat distribution applied to the porous surface. At low channel temperatures, all applied power is. At higher temperatures, the absorbed power decreases linearly from the value shown in this plot to account for evaporation.

account for this in our model, we apply a linear correction to the gaussian such that at 880°C, the heat flux reaches $0MW/m^2$. This means that in our model, when the temperature of a point on the divertor reaches 880°C, that point can no longer absorb heat because all additional incident heat at that point goes into evaporating lithium.

B. Mesh sizing

The mesh provides the set of points at which the ANSYS solver evaluates the MHD equations. It's important to choose an appropriate mesh because a coarse mesh may give an inaccurate solution, while an overly fine mesh will make the solver slow to converge. MHD channel flows generally have thin boundary layers[4] so we used high mesh densities near the edges of the channel (Figure 2) to resolve the boundaries and low mesh densities elsewhere to prevent excessive slowdown.

We tested 3 different mesh densities to find one with the best combination of speed and accuracy. For this test, we used the case where all walls are insulating and there is no current passed through the channel. We found the average velocity over a 2D cross section of the channel and compared the results with an analytical solution from Shercliff[3]:

$$v_0 = \frac{\rho g a^2}{M\eta}\left[1 - \frac{0.852a}{\sqrt{M}b} - \frac{1}{M}\right]. \quad (1)$$

These results are shown in Figure 4. Other studies[4] have found that 2 or 3 nodes in the

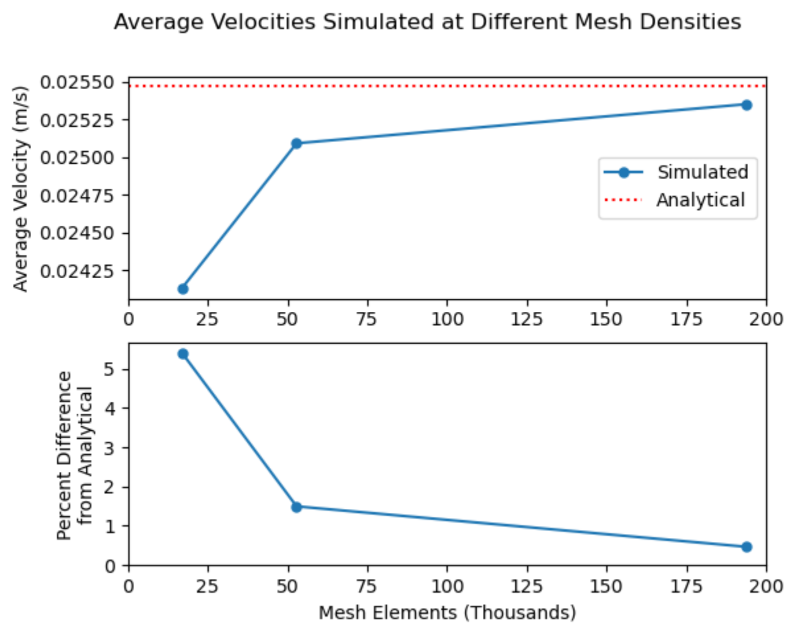

FIG. 4: The upper plot shows the average velocities calculated by ANSYS at several mesh densities. The lower plot shows the percent difference between those velocities and the velocity calculated by Shercliff[3] (Equation 1), which is displayed as the dotted line in the upper plot as well. It seems that as mesh density increases, the simulation is converging towards the analytical solution.

boundary layer give good accuracy, but we found that our setup required 20 or more. While the finest mesh gave the best accuracy, it took nearly a week reach convergence. So, we chose to use the intermediate mesh density because the solution converged within 1 day and was accurate within 2%. To move up to three dimensions, we used 100 mesh elements along the length of the channel. More elements were not necessary because there are no velocity gradients along the length of the channel.

C. Divided simulation and assumption

Since it took 1 day for the solution to converge on a 2D cross section of the channel, it would take months to solve directly for the velocity over the whole channel and even longer to solve for velocity and heat transfer simultaneously. In order to increase speed, we split up the simulation into 3 steps. The ANSYS workbench project that controls the steps is shown in Figure 5. The first step simulates velocity on a 2D cross section of the channel with a certain applied current and no heat applied. The second step takes the 2D velocity profile and applies it to the whole channel. Since there should be translational symmetry along the length of the channel, this step only needs to run a few iterations to smooth the solution out; all of the hard work was already done by the first step. Heat is then introduced in the third step. Since the full velocity solution was already found, the solver only needs to solve the heat transfer equations on a fixed velocity field.

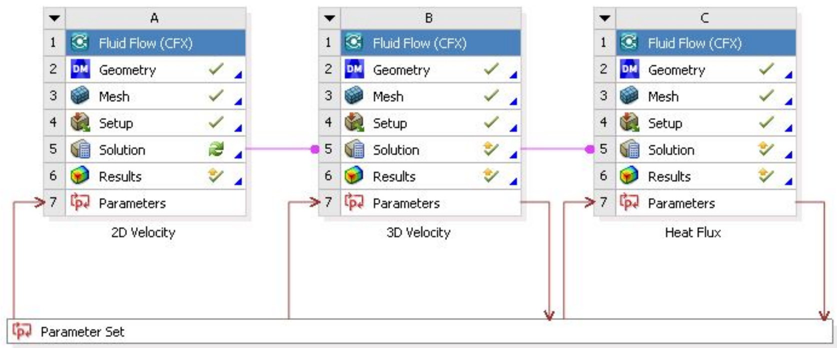

FIG. 5: ANSYS Workbench setup. The 3 blocks calculate a 2D velocity profile, the 3D velocity field, and then heat transfer on the frozen velocity field. All three blocks pass parameters back and forth with the parameter set block, which allows the same setup to evaluate different currents and channel geometries.

This worked well to speed up the simulation. It took only two days, rather than several months, to get a full velocity and heat transfer solution for a given current. However, splitting the simulation up requires the assumption that velocity and heat transfer are independent. This isn't strictly true because electrical conductivity, viscosity, density, etc. of liquid lithium are functions of its temperature[5]. As long as these effects remain small, our simulation should still be a good representation of the system.

III. MODEL VALIDATION

We checked the validity of our model with comparisons to several analytical solutions. First, the velocity profile along the center of the channel parallel to the applied magnetic field should agree with Hartmann's solution[3]:

$$v_z = v_1 \frac{\cosh M - \cosh Mz/a}{\cosh M - (\sinh M)/M}. \tag{2}$$

In Figure 6 we see good agreement between our simulation and this analytical result. The simulation finds the predicted steep boundary layer and nearly constant core flow. Shercliff[3], building on Hartmann's work, predicted a wider boundary layer along the sides parallel to the magnetic field. This is also replicated in our simulation.

Hunt[67] derived the effect of an applied current on average flow velocity in the channel. In Chiang's notation[8], the nondimensionalized mass flow rate is:

$$Q = 2(P + J)\left[2L - 1.911\frac{1}{\sqrt{M}}\right]. \tag{3}$$

Or, using the J factor, J^* as defined in Table I,

$$Q = 2P(1 + J^*)\left[2L - 1.911\frac{1}{\sqrt{M}}\right]. \tag{4}$$

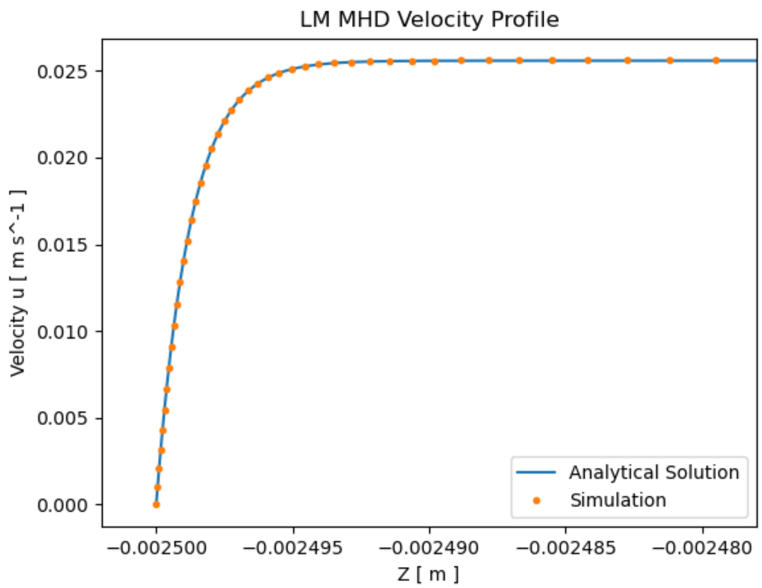

FIG. 6: Comparison between the simulated velocity profile and Hartmann's result (Equation 2) shows good agreement. This is only a small portion of the width of the channel because the boundary layer is thin (approximately $1/M$ of the width of the channel[3]) and the flow is dominated by the uniform core flow

This result is compared with the result of our simulation in Figure 7. Again, we see good agreement between the analytical solution and simulation. At large currents, there is some divergence between the two results. This is because the analytical solution assumes that the top and bottom walls of the channel are perfectly conducting, while in our model they had the same conductivity as the liquid lithium.

IV. RESULTS

A. General considerations

In general, we see that passing a large current through the channel causes a large velocity, which decreases the temperature because the applied heat is being removed more effectively. Specifically, we see that for a J factor of 256 (which corresponds to about 600A/m for the square channel) the outlet temperature is around 300°C and even the maximum temperature is nearing 450°C. This is nearing the range where lithium evaporation is expected to have a small effect on reactor efficiency[2]. This decrease in temperature with increased current is shown for all aspect ratios we tried in Figure 8.

While it's good to see low temperatures at high currents, temperature is really a proxy for what we really care about: how much heat the lithium channel is able to remove from the divertor's plasma facing surface. In Figure 9, we see that at low currents, a fraction of the heat applied is absorbed by the channel. This indicates that large portions of the

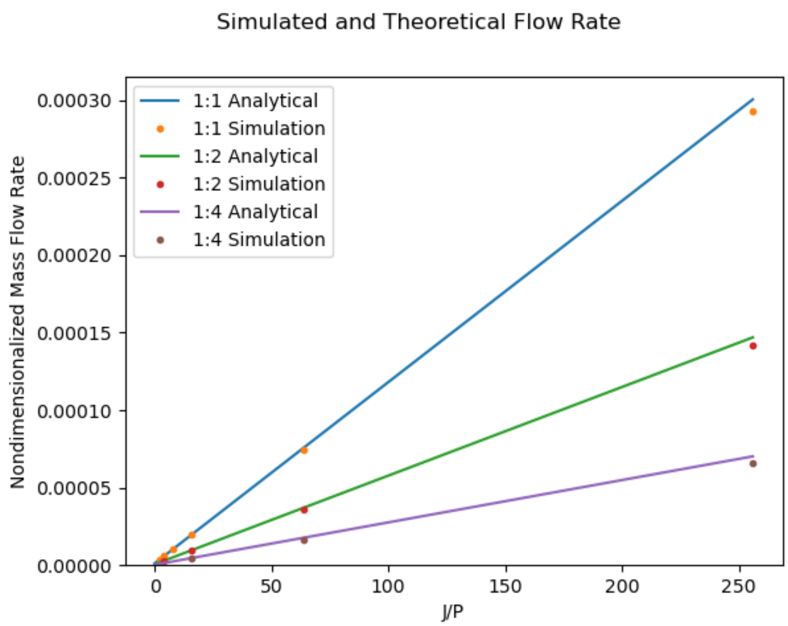

FIG. 7: Comparison between simulated and analytical flow rates as a function of applied current for 3 different aspect ratios. The difference at large currents is due to the conductivity of the electrodes, which is assumed infinite in the analytical solution.

incident heat is lost to lithium evaporation. Once the J factor is over 50, nearly all of the heat is being carried away by the flow rather than by evaporation.

Increasing the current enough to remove the applied heat and prevent the channel's temperature from getting too high is important, but Figure 9 also shows that too much current will be bad for the divertor operation. Joule heat increases quadratically with current, so as applied current increases, the temperature decreases, but the efficiency also decreases because a greater portion of the heat that the liquid needs to carry away is being generated within the channel itself. Taking the square channel as an example, at J factor = 256, nearly 4% of the total heat removed by the channel is generated by the current. At some high current, this effect will get too large and the channel will no longer be able to shuttle away all the heat generated in the lithium.

In order to decrease the temperature down to 450C, higher currents will be needed, but Joule heat also needs to be controlled to keep the divertor's efficiency high.

B. Dependence on Aspect Ratio

At low currents, the larger aspect ratio reduces temperature much more effectively. This makes sense because the larger aspect ratio channels have a greater mass flow rate at similar average velocities. However, as seen in Figure 8, at higher currents, the 1:2 aspect ratio actually reduces maximum temperature slightly more than the 1:1 aspect ratio. At even higher currents, it looks like the 1:4 aspect ratio may reduce the maximum temperature even more, but this would need to be tested by trying even higher currents.

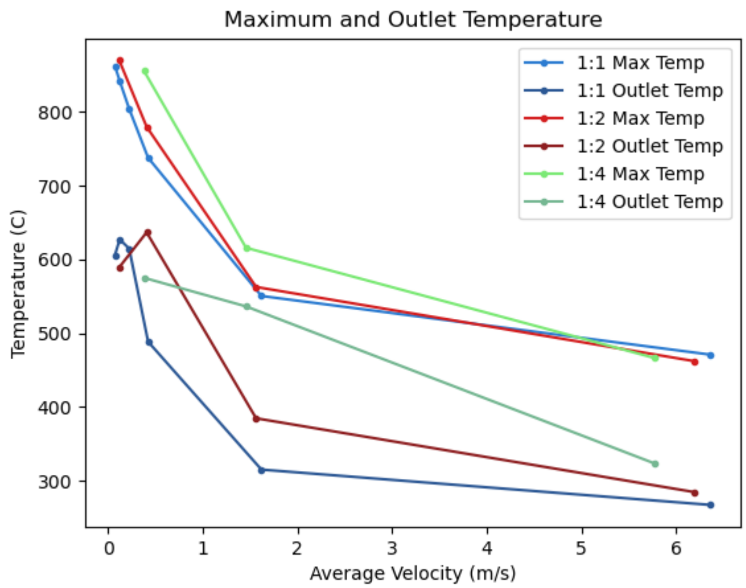

FIG. 8: Maximum temperature and temperature averaged over the channel outlet as a function of increasing flow velocity. This shows that increasing current and flow velocity does decrease the channel temperature. The outlet temperature is always higher for smaller aspect ratios, even at the same flow velocity. Maximum temperature is also higher for small aspect ratios at small currents, but lower for small aspect ratios at large currents. This shows that small aspect ratio channels can remove heat from the hottest part of the channel quickly, even with less coolant than the large channels.

It seems counterintuitive that a small channel could remove heat more effectively than a larger one because the smaller aspect ratio channels have less fluid to carry the heat. As the channel geometries are identical aside from aspect ratio and boundary layer profiles are nearly independent of aspect ratio, it's not clear why this happens.

Referring back to Figure 9, we also see that at flow velocities of several meters per second, the low-aspect ratio channels remove just as much applied heat at the larger-aspect ratio channel, and the thin channels are more efficient because they generate less Joule Heat.

V. CONCLUSION

The goal of this project was to create an ANSYS model that calculates the flow velocities and heat transfer properties of a tokamak divertor porous liquid lithium delivery system. The velocity profiles in our model match analytical solutions for similar systems, which gives us confidence that it's working properly. We also found appropriate mesh densities and a simulation breakdown that allows for heat transfer solutions to be calculated quickly.

In our preliminary analysis of the model, we found that a porous delivery system with liquid lithium channels driven by MHD pumping seems like a feasible way to remove heat from a divertor surface. Our results show that a J factor $J^* > 50$ will be required to get

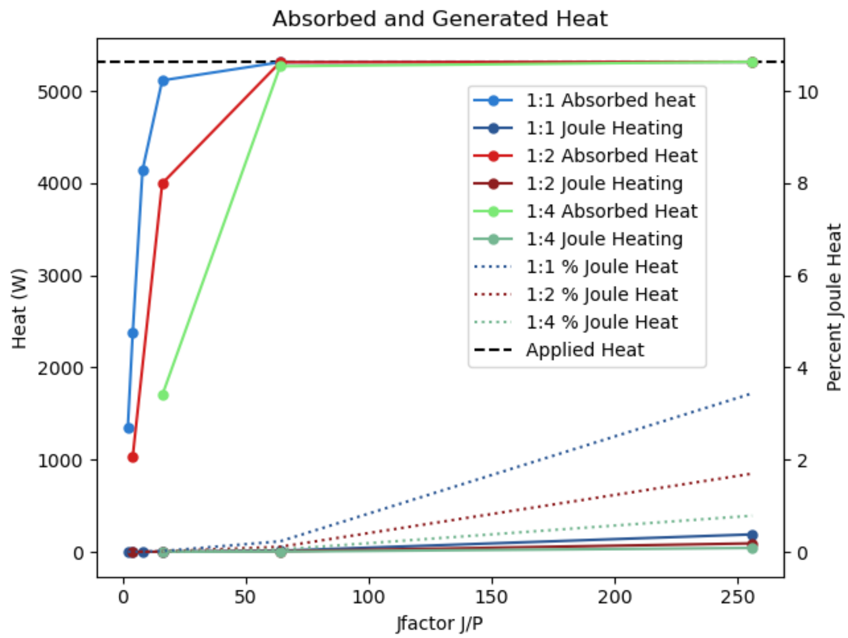

FIG. 9: Absorbed heat and Joule heat as a function of increasing current. All aspect ratios absorb nearly all the incident heat at large enough currents. However, the largest aspect ratio channels generate more joule heat and thus are less efficient than the smaller channels (as seen in the dotted lines).

sufficient liquid lithium velocities to absorb all the applied heat. They also indicate that if large currents are passed through the channel, decreasing the height of the channels may increase efficiency and decrease maximum channel temperature.

Future models will need to account for more realistic, curved divertor geometries. More complexities in the lithium evaporation and porous zone should also be considered. Since the results from this paper can't be generalized to all tokamak divertors, the model itself must be adapted to the constraints of a particular tokamak. This will allow the model to illuminate whether a porous liquid lithium divertor will help that particular tokamak achieve desirable plasma properties and efficient fusion.

ACKNOWLEDGMENTS

Thanks to Dr. Andrei Khodak for his mentorship throughout this project.

This work was made possible by funding from the Department of Energy for the Summer Undergraduate Laboratory Internship (SULI) program. This work is supported by the US DOE Contract No. DE-AC02-09CH11466.

REFERENCES

[1]A. Hassanein, V. Sizyuk, G. Miloshevsky, and T. Sizyuk, "Can tokamaks pfc survive a single event of any plasma instabilities?" Journal of Nuclear Materials **438**, S1266 – S1270 (2013), proceedings of the 20th International Conference on Plasma-Surface Interactions in Controlled Fusion Devices.

[2]T. D. Rognlien and M. E. Rensink, "Impurity transport in edge plasmas with application to liquid walls," Physics of Plasmas **9**, 2120–2126 (2002).

[3]J. A. Shercliff, "Steady motion of conducting fluids in pipes under transverse magnetic fields," Mathematical Proceedings of the Cambridge Philosophical Society **49**, 136–144 (1953).

[4]A. Sterl, "Numerical simulation of liquid metal mhd flows in rectangular ducts," Journal of Fluid Mechanics **216**, 161–191 (1990).

[5]L. Golubchikov, V. Evtikhin, I. Lyublinski, V. Pistunovich, I. Potapov, and A. Chumanov, "Development of a liquid-metal fusion reactor divertor with a capillary-pore system," Journal of Nuclear **233-237**, 667–672 (1996).

[6]J. C. R. Hunt, "Magnetohydrodynamic flow in rectangular ducts," Journal of Fluid Mechanics **21**, 577–590 (1965).

[7]J. C. R. Hunt and K. Stewartson, "Magnetohydrodynamic flow in rectangular ducts. ii," Journal of Fluid Mechanics **23**, 563–581 (1965).

[8]D. Chiang and T. Lundgren, "Magnetohydrodynamic flow in a rectangular duct with perfectly conducting electrodes," Zeitschrift für angewandte Mathematik und Physik ZAMPs **18**, 92–106 (1967).